Macromolecules
ARTICLE

Macromolecules **2010**, *43*, 271–281 **271**
DOI: 10.1021/ma901913f

Synthesis of Ternary, Hydrophilic−Lipophilic−Fluorophilic Block Copolymers by Consecutive RAFT Polymerizations and Their Self-Assembly into Multicompartment Micelles

Katja Skrabania,[†] Hans v. Berlepsch,[‡] Christoph Böttcher,*[,‡] and André Laschewsky*[,†,§]

[†]*Department of Chemistry, Universität Potsdam, Karl-Liebknecht-Str. 24-25, D-14476 Potsdam-Golm, Germany,* [‡]*Forschungszentrum für Elektronenmikroskopie, Institut für Chemie und Biochemie, Freie Universität Berlin, Fabeckstr. 36a, D-14195 Berlin, Germany, and* [§]*Fraunhofer Institute for Applied Polymer Research, D-14476 Potsdam-Golm, Germany*

Received August 28, 2009; Revised Manuscript Received October 10, 2009

ABSTRACT: Linear amphiphilic diblock and ternary triblock copolymers were synthesized by the RAFT method in three successive steps, using oligo(ethylene oxide) monomethyl ether acrylate, butyl or 2-ethylhexyl acrylate, and 1*H*,1*H*,2*H*,2*H*-perfluorodecyl acrylate. The diblock and the triblock copolymers, which consist of a hydrophilic, a lipophilic, and a fluorophilic block, self-assemble in water into spherical micellar aggregates. Imaging by cryogenic transmission electron microscopy (cryo-TEM) revealed that the cores of the micellar aggregates made from these "triphilic" copolymers undergo local phase separation to form various ultrastructures, which depend sensitively on the given block sequence. While the sequence hydrophilic−lipophilic−fluorophilic resulted in multicompartment cores with core−shell−corona morphology, the sequence lipophilic−hydrophilic−fluorophilic provided new "patched double micelle" and larger "soccer ball" structures.

Introduction

In biological systems, such as cells, enzymes, transport proteins, etc., distinct functional and structural units coexist and perform in close proximity without mutual interference. They may even cooperate to achieve mutual synergies. In the context of biomimicking and bioinspired materials, the concept of multicompartment core micelles was thus derived by H. Ringsdorf in the 1990s,[1,2] in order to obtain stable colloids with coexisting distinctly different hydrophobic domains, in analogy to certain transport proteins in the blood such as serum albumin.[3,4] Micellar aggregates of amphiphilic block copolymers are an attractive platform for such multicompartment core micelles, by virtue of the structural diversity and stability of the aggregates formed.[5−8] However, classical amphiphilic block copolymers, such as poly(ethylene oxide-*block*-propylene oxide) or poly(styrene-*block*-methacrylic acid), exhibit only one single, structurally undifferentiated type of hydrophobic domain in their micelles.

Since then, a few research groups have tackled this topic by different approaches. A key feature is the induction of microphase separation within the hydrophobic region in order to compartmentalize the micellar core. Moreover, the chemical nature of these compartments has to differ substantially so that they can for instance selectively solubilize low molar mass guests. As this profile is difficult to achieve with hydrocarbon-based polymers exclusively, most approaches have focused on the combination of hydrocarbon and fluorocarbon hydrophobic segments,[3] which are poorly compatible with each other. The problem has increasingly incited theoretical work and simulations[9−17] to learn about the influence of molecular architecture, block length, and polymer concentration on the micellar morphologies.

Still, as the mentioned requirements are difficult to meet, only few experimental studies have dealt with multicompartment micelles so far.[3,18−34] The first approaches toward multicompartment micelles relied on polysoap systems.[18,19,22,24,34] Indeed, selective solubilization in the lipophilic and fluorophilic compartments could be shown.[18,23,24] Nonetheless, it has not been possible yet to visualize the multicompartment character of these systems e.g. by cryogenic transmission electron microscopy (cryo-TEM). While the differences in the electron density of fluorocarbons and hydrocarbons are strong enough to be differentiated by electron microscopy, it seems that the different domains in these systems are probably too small to be resolved.

An alternative strategy toward multicompartment micelles is based on amphiphilic block copolymers composed of one hydrophilic and two hydrophobic blocks, one being lipophilic and the other being fluorophilic. As the coherent lipophilic and fluorophilic segments in such block copolymers are inherently larger compared to polysoaps, microdomains can be formed, which pass resolution limit. Particularly successful has been the use of ABC miktoarm block copolymers based on poly(ethylene oxide) (PEO), poly(ethylethylene), and poly(perfluoropropylene oxide).[25,26,29,35−38] The emerging new morphology was referred to as a "hamburger" micelle due to its shape[38] and showed good solubilization for hydrocarbon as well as fluorocarbon probes.[26] Nonetheless, the synthesis of these structures is painstaking,[35] and the strategy can be hardly generalized to blocks of other chemical nature. Also, the miktoarm star architecture inherently fixes the relative positions of the blocks to each other. In contrast, linear terblock copolymers dispose of an additional structural parameter, namely the variation of the block sequence.[39] Still, the self-assembly of linear triphilic block copolymers containing a fluorocarbon block has been rarely reported. For a long time, such polymers had to be prepared by living ionic

*To whom correspondence should be addressed: Tel +49 30 838 54934, Fax +49 30 838 56589, e-mail christoph.boettcher@fzem.fu-berlin.de (C.B.); Tel +49 331 977 5225, Fax +49 331 977 5036, e-mail laschews@rz.uni-potsdam.de (A.L.).

Published on Web 11/06/2009

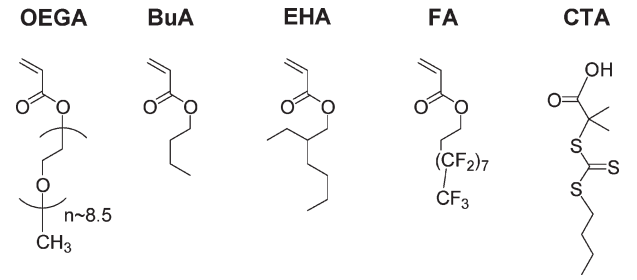

Figure 1. Monomers and RAFT agent used for the synthesis of triphilic ABC block copolymers.

polymerization,[21,40,41] thus limiting severely the choice of suited monomers. A simplified triblock copolymer analogue e.g. was prepared by end-capping oligomeric poly(2-methyl-2-oxazoline) with a hydrocarbon and a fluorocarbon group, respectively, for which ^{19}F NMR relaxation experiments suggested the separation of hydrocarbon and fluorocarbon microdomains.[21] However, results suggested that rather two populations of homogeneous microdomains were formed instead of coherent multicompartment structures.[30,41] Important progress was made by applying controlled free radical polymerization (CRP) methods[42,43] for the synthesis of such triphilic copolymers, as a much larger pool of monomer building blocks can be employed. For instance, cationic triphilic block copolymers prepared by CRP methods were shown to form small micelles with a sphere-on-sphere multicompartment morphology, as revealed by cryo-TEM.[27] Still, the hydrophobic blocks of this polymer have high glass transition temperatures T_g, resulting in micelles with a "frozen" core[44−46] a priori less suited to solubilize guest molecules. Hence, we recently developed linear triphilic block copolymers containing hydrophobic blocks with low glass transition temperatures T_g using the RAFT technique.[32] These polymers consist of a linear PEO chain as hydrophilic block anchored to lipophilic blocks such as poly(butyl acrylate) (polyBuA) or poly(2-ethylhexyl acrylate) (polyEHA) and to a fluorophilic block such as poly(1*H*,1*H*,2*H*,2*H*-perfluorodecyl acrylate) (polyFA). These compounds formed micelles with unique multicompartment cores exhibiting directly visible lamellar fluorocarbon domains. As the synthetic strategy was based on the use of a PEO-based macro-chain-transfer agent, the block sequence was fixed such that the hydrophilic block was in the end terminal position. The limited length of the PEO block (molar mass 5000 g mol^{-1}) implied the use of only short hydrophobic chains, in order to maintain a sufficient hydrophilic−hydrophobic balance of the nonionic block copolymers and thus to obtain stable colloids in aqueous media.[47,48] Now, we extend these studies by synthesizing and investigating linear triphilic block copolymers, in which the PEO block is replaced by a hydrophilic block based on oligoethylene glycol acrylate (OEGA) macromonomers, employing three successive RAFT polymerization steps. The various monomers and the low molar mass RAFT agent used in the first step are depicted in Figure 1. On the one hand, the high water affinity of the nonionic hydrophilic block enables the use of longer hydrophobic blocks than previously reported. On the other hand, this approach allows to vary the block sequence and thus to study also triphilic copolymers, in which the hydrophilic block is not in the terminal but in the central position.

Experimental Section

Materials. The synthesis of RAFT agent 2-(butylsulfanylthiocarbonylsulfanyl)-2-methylpropionic acid (CTA) under phase transfer catalysis conditions[49] was described before.[32] The reference compound 2-(butylsulfanylthiocarbonylsulfanyl)propionic acid butyl ester (BTP) was synthesized adapting a literature procedure,[50] as specified in the Supporting Information. Oligo(ethylene oxide) monomethyl ether acrylate (OEGA, Aldrich, M_r = 454 g mol^{-1}) and 1*H*,1*H*,2*H*,2*H*-tetrahydroperfluorodecyl acrylate (FA, Aldrich) were filtered over a column with basic alumina (Merck, activity I, 0.063−0.200 mm) to remove the inhibitor and possible traces of oligomers prior to polymerization. Monomers *n*-butyl acrylate (BuA, Acros) and 2-ethylhexyl acrylate (EHA, Acros) were purified by vacuum distillation from CaH_2 and stored at −20 °C under N_2 in the dark. 2,2′-Azobis(isobutyronitrile) (AIBN, Acros, 98%) was recrystallized from methanol. Initiators V-501 (4,4′-azobis(4-cyanopentanoic acid)) and V-40 (1,1′-azobis-(cyclohexane-1-carbonitrile)) were gifts from Wako and used as received. THF (Merck, extra pure) was distilled from Na/K to remove the inhibitor and peroxides. Toluene (Acros, p.a.), and α,α,α-trifluorotoluene (TFT, Acros, 99+%) were used as received. Dialysis tubes "ZelluTrans" (Roth, Germany) had a nominal molar mass cutoff of 4000−6000 Da.

Synthesis of the Homopolymers and Block Copolymers. The experimental conditions for the synthesis of the amphiphilic ABC triblock copolymers and their precursors are specified in the Supporting Information (Table S1). Conversions were estimated gravimetrically based on the amount of recovered polymer after purification. All polymers were characterized by ^{1}H NMR spectroscopy, SEC, and UV−vis spectroscopy. The data of their composition and molar mass characterization are summarized in Table 1.

Synthesis of the Hydrophobic MacroCTA $(EHA)_{120}$. CTA (137 mg, 5.43×10^{-4} mol), 2-ethylhexyl acrylate (20 g, 109 mmol), and initiator AIBN (8.9 mg, 5.43×10^{-5} mol) in toluene (60 g) were deoxygenated by purging with N_2 for 45 min, and the mixture was stirred for 4 h at 65 °C. The polymerization was stopped by cooling the flask rapidly in a dry ice/acetone mixture. The polymer was isolated by precipitation into cold methanol; the obtained yellow gluey precipitate was washed several times with methanol, dissolved in benzene, and lyophilized to give 11.2 g of a bright yellow, viscous, gluey paste.

Synthesis of Hydrophilic MacroCTAs. In a typical procedure, OEGA (19.8 g, 43.6 mmol), CTA (4.36×10^{-4} mol), initiator V-501 (6.2 mg, 2.2×10^{-5} mol), and a mixture of deionized water and methanol (60 g, 1:1 by wt) were deoxygenated by purging with N_2 for 45 min and then stirred for 2 h at 69 °C. The polymerization was stopped by cooling the flask rapidly in a dry ice/acetone mixture. Unreacted macromonomer was removed by dialysis against deionized water for 5 days. The obtained aqueous solution was lyophilized to give macroCTA $(OEGA)_{65}$ as bright yellow, viscous paste.

Synthesis of Amphiphilic Di- and Triblock Copolymers. The reaction conditions and the engaged amounts of particular macroCTAs, monomers, initiator, and solvents can be found in the Supporting Information (Table S1).

In a typical procedure for the synthesis of diblock copolymers, macroCTA $(EHA)_{120}$ (4.0 g, 1.91×10^{-4} mol), monomer OEGA (18.6 g, 41 mmol), AIBN (3.1 mg, 1.91×10^{-5} mol), and toluene (110 g) were deoxygenated as described above and stirred for 2.5 h at 65 °C. The polymerization was stopped by cooling the flask rapidly in a dry ice/acetone mixture. The solvent was evaporated, the residue redissolved in THF, and the unreacted macromonomer removed by dialysis against deionized water (nominal molar mass cut off 4000−6000 Da) for 5 days. With ongoing solvent exchange, the solution turns into a milky emulsion. After filtration, the emulsion was lyophilized to give 8 g of diblock copolymer as a yellow paste, which can be directly dissolved in water to form opaque solutions.

In a typical procedure for the synthesis of triblock copolymers, diblock macroCTA $(EHA)_{120}$-$(OEGA)_{50}$ (2.0 g, 4.26×10^{-5} mol), monomer FA (0.94 g, 1.81 mmol), and AIBN (1.6 mg, 9.7×10^{-6} mol) in α,α,α-trifluorotoluene (TFT) (15 g) were deoxygenated by purging with N_2 for 20 min and stirred for 19 h at 65 °C. The polymerization was stopped by cooling the flask

Table 1. Characterization of Triphilic ABC Triblock Copolymers and Their Precursors

	M_n (kg mol^{-1})				M_w/M_n	wt % FA	
sample[a]	theory[b]	UV[c]	NMR[d]	SEC[e]	SEC	IC[f]	NMR[g]
$(OEGA)_{70}$	28	32		8	1.2		
$(OEGA)_{85}$	21	39		12	1.2		
$(EHA)_{120}$	21	22		15	1.3		
$(OEGA)_{70}$-$(BuA)_{83}$	41	53	42	13	1.3		
$(OEGA)_{70}$-$(EHA)_{140}$	45	78	58	15	1.5		
$(OEGA)_{85}$-$(FA)_{24}$	44	59	51	13	1.2		
$(EHA)_{120}$-$(OEGA)_{50}$	45	47	45	13	1.3		
$(EHA)_{120}$-$(OEGA)_{109}$	82	80	72	10	1.4		
$(OEGA)_{70}$-$(BuA)_{83}$-$(FA)_{13}$	60	74	49	14	1.3	18	14
$(OEGA)_{70}$-$(EHA)_{140}$-$(FA)_{13}$	—[h]	165	64	16	1.4	10	11
$(EHA)_{120}$-$(OEGA)_{50}$-$(FA)_{40}$	—[h]	73	66	14	1.3		32
$(EHA)_{120}$-$(OEGA)_{109}$-$(FA)_{25}$	88	—[i]	85	12	1.4	18	15

[a] Degrees of polymerization (DP) according to combined UV and NMR data (see footnote [d]). [b] Number-average molar mass M_n theoretically expected from the obtained yield, when taking yield for conversion and assuming 100% end-group functionalization. [c] Calculated by UV spectroscopic end-group analyis based on $\pi-\pi^*$ thiocarbonyl absorption band of reference BTP at λ_{max} = 307 nm (ε = 14 400 L mol^{-1} cm^{-1} in CH_2Cl_2). [d] M_n of di- and triblock copolymers calculated from averaged compositional data according to ^{1}H NMR spectroscopy, assuming that M_n(UV) of the first block is preserved in the block copolymers. [e] Polystyrene equivalent molar mass and PDI according to SEC, apparent values only. [f] Determined by fluoride ion chromatography after combustion. [g] Determined via ^{1}H NMR spectra from signal of ester α-methylene protons (cf. Figure 2, signal "f"). [h] Due to material lost during purification calculation of M_n(theory) from the yield not conclusive. [i] Loss of trithiocarbonate groups; end-group analysis not conclusive.

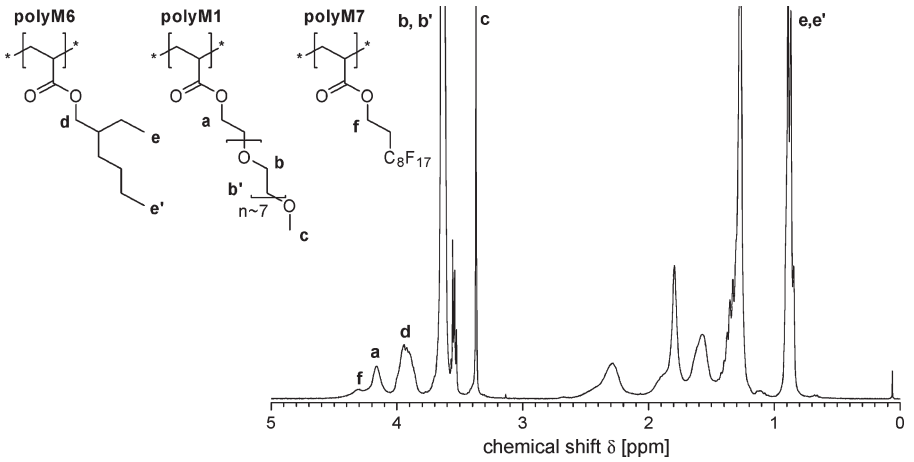

Figure 2. ^{1}H NMR spectrum of polymer $(EHA)_{120}$-$(OEGA)_{50}$-$(FA)_{40}$ in $CDCl_3$.

rapidly in a dry ice/acetone mixture. The reaction mixture foamed strongly upon shaking. After removing most of the solvent by rotary evaporation, unreacted monomer FA was removed by dialysis against ethanol for 3 days. The dialysis bags were swollen in deionized water prior to dialysis against ethanol. Then, the polymer solution was dialyzed against deionized water to remove ethanol, filtered, and lyophilized.

Preparation of Micellar Solutions. Micellar solutions of amphiphilic triblock copolymers were prepared starting from a common solvent, applying two different procedures. In procedure A, 50 mg of block copolymer were dissolved in THF (20 g). The solutions were stirred for at least 1 h to ensure complete dissolution. Then, 10 g of purified water (resistance of 18 MΩ cm^{-1}) were added dropwise under stirring to induce the formation of aggregates. The excess of THF was slowly evaporated at ambient conditions, and the concentration of the solution was adjusted to 0.5 wt %. In procedure B, 25 mg of the block copolymer was dissolved in 10 g of THF and stirred for 1 h at ambient conditions. In a separate vial, 5 g of purified water (resistance of 18 MΩ cm^{-1}) was weighed. The THF solution and the purified water were transferred to a water bath preset to 70 °C. Under stirring, the THF solution was added dropwise to the purified water. After complete addition, the aqueous solution was stirred for 1 h more at 70 °C in order to evaporate residual THF. Finally, the samples were cooled to ambient temperature, and the concentration was adjusted to 0.5 wt %. Additionally, micellar solutions prepared by protocol A were annealed for ca. 3 weeks at 78 °C (protocol C).

Methods. ^{1}H (300 MHz) and ^{19}F NMR (282 MHz) spectra were taken with a Bruker Avance 300 apparatus and referenced to the solvent residual peak. α,α,α-Trifluorotoluene (0.5 wt %, δ = −63.72 ppm vs $CFCl_3$) was used as secondary standard for the chemical shifts in ^{19}F spectra. UV−vis spectra were recorded with a Cary 5000 UV−vis spectrophotometer (Varian) using quartz glass cuvettes (Suprasil, Hellma, Germany). The fluorine contents of the amphiphilic triblock copolymers were determined after combustion in oxygen (Schöniger method) converting the organic fluorine into fluoride, which was quantified by ion chromatography (761 Compact IC apparatus, Metrohm AG, Herisau, Switzerland) equipped with suppressor technology, an autosampler, and an electric conductivity detector. Size exclusion chromatography (SEC) was run in THF at 25 °C (flow rate: 1.0 mL min^{-1}) using a TSP apparatus (Thermo Separation Products from Thermo-Finnigan GmbH, Dreieich, Germany) equipped with a Shodex RI-71 refractive index detector, a TSP UV detector (260 nm), and a set of PSS SDV columns (styrene/divinylbenzene, 100 and 1000 Å porosity, 5 μm particle size) and calibrated with polystyrene standards (PSS GmbH Mainz, Germany). Thermal properties of the amphiphilic polymers were measured with a TGA/SDTA 851 thermal gravimetric analyzer (TGA) (Mettler Toledo) and a DSC 822 differential scanning calorimeter (DSC) (Mettler Toledo) under a nitrogen

atmosphere, with heating and cooling rates of 10 and 20 K min^{-1}.

Dynamic light scattering (DLS) was performed at a scattering angle $\theta = 173°$ ("backscattering detection") with a high-performance particle sizer (HPPS-ET, from Malvern Instruments, UK) equipped with a He−Ne laser ($\lambda = 633$ nm) and a thermoelectric Peltier element (temperature control range 10−90 °C) as described in detail before.[51] The autocorrelation functions were analyzed with the CONTIN method. Apparent mean hydrodynamic diameters D_h (according to volume distribution) of micelles or aggregates were calculated according to the Stokes−Einstein equation, $D_h = kT/3\pi\eta D_{app}$, with D_{app} being the apparent diffusion coefficient and η the viscosity of the solution. Prior to measurements, the polymer solutions were filtered through a WICOM OPTI-Flow 0.45 μm disposable filter.

Samples for cryo-TEM measurements were prepared at room temperature by placing a droplet (5 μL) of the solution on a hydrophilized perforated carbon film Quantifoil grid (60 s plasma treatment at 8 W using a BALTEC MED 020 device). The excess fluid was blotted off to create an ultrathin layer (typical thickness of 100 nm) of the solution spanning the holes of the carbon film. The grids were immediately vitrified in liquid ethane at its freezing point (−184 °C) using a standard plunging device. Ultrafast cooling is necessary for an artifact-free thermal fixation (vitrification) of the aqueous solution avoiding crystallization of the solvent or rearrangement of the assemblies. The vitrified samples were transferred under liquid nitrogen into a Philips CM 12 transmission electron microscope using a Gatan cryo holder and stage (model 626). Microscopy was carried out at −175 °C sample temperature using the microscope's low-dose mode at a primary magnification of 58 300. The acceleration voltage was 100 kV, and the defocus was chosen to be 1.5 μm.

Results and Discussion

Synthesis and Molecular Characterization of the Polymers. The ternary block copolymers were prepared in three consecutive RAFT polymerization steps, starting with the unsymmetrical, monofunctional trithiocarbonate 2-(butylsulfanylthiocarbonylsulfanyl)-2-methylpropionic acid (CTA). While the trithiocarbonate moiety should minimize retardation effects in the polymerization of acrylates,[52] the 2-carboxyprop-2-yl group is a good homolytic leaving group, which was reported to give good control of the polymerization of acrylic and styrenic monomers.[49] In order to minimize losses of the RAFT active end-groups, polymerizations were stopped at about 50% conversion. A major difficulty in the synthesis, purification, and molecular analysis of the ternary block copolymers turned out to be the selection of suitable solvents due to the disparate solubilities and poor compatibilities of the individual blocks. In fact, highly fluorinated polymers are rarely soluble in conventional organic solvents.[53] While polyFA can be readily dissolved in fluorinated compounds, such as hexafluorobenzene or hexafluoroisopropanol, these are nonsolvents for the aspired hydrophilic and lipophilic blocks. In order to minimize these difficulties, the syntheses of amphiphilic triblock copolymers were started with the hydrophilic or the lipophilic block. Still, the reaction solvents had to be adapted individually for each case (see Supporting Information, Table S1). Because of the solubility problems, the fluorinated block was synthesized for all prepared triblock polymer samples in the last polymerization step employing α,α,α-trifluorotoluene as reaction medium. Because of the low reactivity of FA,[32] copolymerizations of the fluorinated block were carried out at 65 °C for a prolonged time to attain nearly full conversions. The purification of the block copolymers was difficult, as nonsolvents for one block are often good solvents for the other. As various attempts to precipitate the copolymers resulted in stable milky dispersions only, they were purified by several dialysis steps. Noteworthy, the diblock and triblock copolymer solutions remained transparent upon dialysis against ethanol, although ethanol is a nonsolvent for polyFA and dissolves polyEHA only partially. When these solutions were finally dialyzed against water, bluish or turbid aqueous solutions were obtained, but no macroscopic phase separation occurred. This is a first evidence for the successful formation of di- and triblock copolymers with high blocking efficiency.

The synthesized macroCTA homopolymers were characterized by SEC, ^{1}H NMR spectroscopy, and end-group analysis via UV spectroscopy (Table 1) to determine their molar mass, molar mass distributions, and the presence of RAFT active end-groups and to confirm the absence of residual monomer. SEC showed mononodal, relatively narrow molar mass distributions, but the apparent molar mass values based on the calibration with polystyrene standards are approximate only in the case of polyEHA and even strongly misleading in the case of the polyOEGA due to its comblike architecture.[54] The concentration of RAFT active end-groups could not be determined by ^{1}H NMR spectroscopy, because either the proton signals of the employed CTA coincide with those of the polymers, and/or as the relative amount of end-groups is too small to be determined precisely due to the high molar mass of polyOEGA samples. Consequently, the thiocarbonyl end-groups were quantified by UV spectroscopy using the molar absorptivity of the low molar mass reference compound butyl 2-(butylsulfanylthiocarbonylsulfanyl) propionate (BTP) assuming one active end-group per polymer molecule.

Unfortunately, the amphiphilic and associative character of the diblock and triblock copolymers hampered their meaningful analysis by size exclusion chromatography, as size exclusion was superposed by adsorption as well as associative phenomena. Hence, the molecular analysis of the block copolymers was based on ^{1}H NMR and UV spectroscopy, proving the removal of any residual monomer and determining the copolymer compositions as well as the concentration of thiocarbonylthio end-groups. Figure 2 exemplifies the ^{1}H NMR spectra of $(EHA)_{120}$-$(OEGA)_{50}$-$(FA)_{40}$. The methylene protons in the α-position to the ester functionalities of the EHA, OEGA, and FA repeat units are sufficiently resolved to allow deconvolution. They were thus used to determine the composition of the block copolymers. Note that $CDCl_3$ is a good solvent for the polymers of OEGA, BuA, and EHA, but not for the homopolymer of FA. Still, the triblock copolymers dissolved completely in $CDCl_3$ and formed transparent solutions. Nevertheless, the fluorinated blocks are probably still associated as suggested by the attenuation/broadening of the respective signals in the ^{1}H NMR and ^{19}F NMR spectra (Figure 3). As the compositional analysis by ^{1}H NMR spectroscopy was not very accurate for the short fluorinated blocks due to their small fraction in the block copolymers, the approximate contents of fluorinated repeating units were verified by elemental analysis. The results obtained by both methods agree reasonably well (Table 1). From the copolymer composition according to the ^{1}H NMR spectra in $CDCl_3$, the molar masses of the diblock and triblock copolymers were calculated, assuming that the molar mass of the first block, which was determined by end-group analysis via UV spectroscopy, remained unchanged in the following copolymerization steps.

The compatibility of the three polymer blocks was investigated in bulk by thermal analysis in order to learn about their compatibilities and possible microphase separation

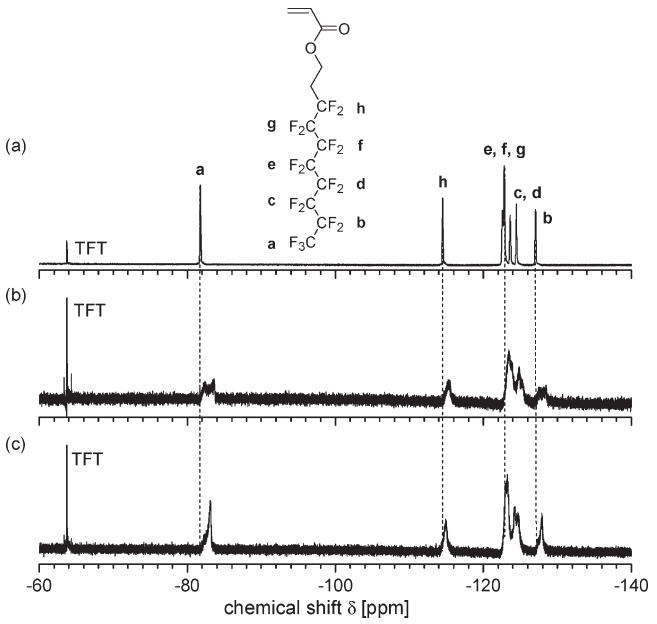

Figure 3. Solvent effects on the ^{19}F NMR spectra of the fluorinated monomer FA and an ABC triblock copolymer containing a polyFA block: (a) monomer FA in $CDCl_3$; (b) $(EHA)_{120}$-$(OEGA)_{50}$-$(FA)_{40}$ in $CDCl_3$; (c) $(EHA)_{120}$-$(OEGA)_{50}$-$(FA)_{40}$ in THF. Internal reference: α,α,α-trifluorotoluene (TFT).

Table 2. Thermal Analysis of Homo- and Triblock Copolymers by Differential Scanning Calorimetry (DSC)

polymer	T_g[a] [°C]	T_r[b] [°C]	T_m[c] [°C]	T_m[d] [°C]
$(OEGA)_{70}$	−62	−44	5	
$(EHA)_{120}$	−65			
$(FA)_n$[e]				77
$(OEGA)_{70}$-$(BuA)_{83}$-$(FA)_{13}$	−65	−37	1	66
$(OEGA)_{70}$-$(EHA)_{140}$-$(FA)_{13}$	−65	−32	0	65
$(EHA)_{120}$-$(OEGA)_{50}$-$(FA)_{40}$	−65	−35	3	63

[a] Glass transition temperature. [b] Recrystallization temperature. [c] First melting temperature. [d] Second melting temperature. [e] Reference sample prepared by free radical polymerization.

between the core-forming hydrophobic blocks. Thermal gravimetric analysis (TGA) showed that the various acrylate homopolymers and block copolymers are thermally relatively stable and undergo degradation only above 250 °C, so that analysis by differential scanning calorimetry (DSC) is feasible without any problem below 150 °C. The results are summarized in Table 2.

All studied triblock copolymers exhibit a glass transition at about −65 °C, a recrystallization peak at −40 to −30 °C, and a broad melting peak around 0 °C (see Supporting Information, Figure S1). These signals are attributed to the hydrophilic polyOEGA block, which superpose the glass transitions of the lipophilic blocks polyBuA and polyEHA, which both are expected in the range of −70 to −50 °C. No glass transition was observed in the temperature range studied for polyFA, as it is semicrystalline (due to its rigid perfluorinated side chains) and shows a sharp melting peak around 75−80 °C (Table 2). Though in the triblock copolymers the melting temperature was slightly decreased, presumably due to the low molar mass of the block, its presence indicates that the fluorophilic block is microphase separated from the other blocks. Similarly, the melting peak of the polyOEGA block demonstrates that this block is also microphase separated from the other blocks. Therefore, the thermal analysis reveals that all polymer blocks are thermodynamically incompatible with each other in bulk. Consequently, these polymers are also expected to microphase separate in selective solvents, thus enabling the formation of micellar aggregates with segregated cores.

Self-Assembly of Amphiphilic Precursors and the Triphilic ABC Block Copolymers in Water. The new triphilic triblock copolymers were anticipated to self-assemble in water as well as in certain organic solvents due to the very disparate affinities of their constituting blocks. In fact, preliminary experiments by dynamic light scattering suggest the association e.g. in $CHCl_3$, but not in THF (see Supporting Information, Table S2). Nonetheless, more detailed studies of the self-assembly of the new diblock and triblock copolymers were restricted to aqueous solutions in this work. Qualitatively, the self-assembly of amphiphilic block copolymers is evident from the ^1H NMR spectra in D_2O, as the signals of the hydrophobic blocks are strongly attenuated or even suppressed due to the strongly reduced mobility of polymer chains within the aggregate cores. Only the characteristic signals of the hydrophilic block are visible (see Supporting Information, Figure S2).

Different from charged amphiphilic block copolymers, the nonionic triblock copolymers were not directly soluble in water due to the lower hydrophilicity of the nonionic block. Therefore, aqueous micellar solutions were prepared starting from a common, water-miscible solvent. After mixing this solution with a large excess of water, the organic solvent is removed by evaporation. Several water-miscible organic solvents were tested as common solvents for the dispersion of the copolymers, such as ethanol, acetone, *N*,*N*-dimethylformamide (DMF), and *N*,*N*-dimethylacetamide (DMAc). All these solvents however were not suited for the dispersion procedure, as they do not dissolve the apolar polyEHA and polyFA blocks. Among the conventional solvents tested, only THF swells the fluorinated block, although it cannot dissolve it. Still, all prepared diblock and triblock copolymers were readily soluble in THF and formed transparent homogeneous solutions. Thus, THF seemed the most suitable common solvent for the dispersion of amphiphilic triblock copolymers in water. DLS studies of these solutions gave no hint for larger associates formed (see Supporting Information, Table S2), but the notable broadening of the ^{19}F NMR signals (Figure 3) may suggest that the fluorophilic blocks might be somehow associated in THF, nevertheless. In particular, the signals at −82 to −84 ppm and at −128 to −130 ppm, which are attributed to the terminal CF_3−CF_2− moiety, appear to be splitted. Such splitted signals have been explained by the coexistence of free and aggregated fluorocarbon chains with slow exchange rates on the NMR time scale.[22,55] Hence, it is not clear whether aggregation in water starts from a state where all block copolymers are dissolved on the molecular level.

Micellar solutions with a final concentration of 0.5 wt % were prepared by two protocols, either by slowly adding water to a solution of the block copolymer in THF at 25 °C (protocol A) or by adding the polymer solutions in THF dropwise to water at 70 °C (Table 3). The polymer concentration in the common solvent THF was kept deliberately low in order to favor the formation of micelles instead of clustered morphologies which have been often reported for higher polymer concentrations.[56,57]

In a first survey, the size of aggregates formed by the block copolymers in water was analyzed by DLS (Table 3). Amphiphilic diblock precursors and triphilic triblock copolymers were thus compared. DLS analysis of the diblock copolymers discloses aggregates with mean hydrodynamic diameters (D_h) in the range of 14−55 nm, which point to the formation of spherical micelles. The colloids show a

Table 3. Characteristics of the Micellar Aggregates of Amphiphilic Di- and Triblock Copolymers As Studied by Cryo-TEM

sample	preperation protocol[a]	D_{core}[b] [nm]	$D_{FC\ domain}$ [nm]	L_{corona} [nm]	$D_{particle}$ [nm]	D_h by DLS[k] [nm]
$(OEGA)_{70}$-$(BuA)_{83}$	A	ca. 13[c]		ca. 18[c]	ca. 31	19
$(OEGA)_{70}$-*b*-$(EHA)_{140}$	A	28		17	45	42
$(OEGA)_{85}$-*b*-$(FA)_{24}$	A	12		13	25	14
$(EHA)_{120}$-$(OEGA)_{50}$	A	29		30	59	55
$(EHA)_{120}$-$(OEGA)_{109}$	A	25		18	43	51
$(OEGA)_{70}$-$(BuA)_{83}$-$(FA)_{13}$	A	16	—[d]	22	38	22
	B	ca. 14[c]	—[d]	ca. 7[c]	21	23
	C	28	11	13	41	
$(OEGA)_{70}$-$(EHA)_{140}$-$(FA)_{13}$	A	32	14	18	50	39
	B	28	ca. 13[e]	27	55	38
	C	34	22	30	64	
$(EHA)_{120}$-$(OEGA)_{50}$-$(FA)_{40}$	A	66	~20/~8[h]	—[g]		240
	B	46	~20/~8[h]	21	67	82
	C	46	~20/~8[h]	—[g]		
$(EHA)_{120}$-$(OEGA)_{109}$-$(FA)_{25}$	A	29[i]	—[j]	30[i]	59	72
	B					119
	C	36	—[j]	16	52	

[a] Micelle preparation by solvent exchange at 25 °C (A) and 70 °C (B); solutions prepared by protocol A after annealing for ca. 3 weeks at 78 °C (C). [b] Number-average mean diameter. [c] Due to very small aggregates and low contrast only approximate values can be given. [d] No segregated FC domains visible. [e] FC domain only partially visible. [g] As the micelles were irregularly packed, the corona thickness (L_{corona}) could not be determined from their interstitial distance. [h] Fluorinated domains are disks which are about 20 nm in diameter and ~8 nm in thickness. [i] Dimensions of irregularly shaped spherical aggregates. [j] Thin FC "caps" partially covering of the micellar core (cf. Figure 9); dimensions difficult to determine due to 2D projection. [k] Mean hydrodynamic diameter according to volume distribution.

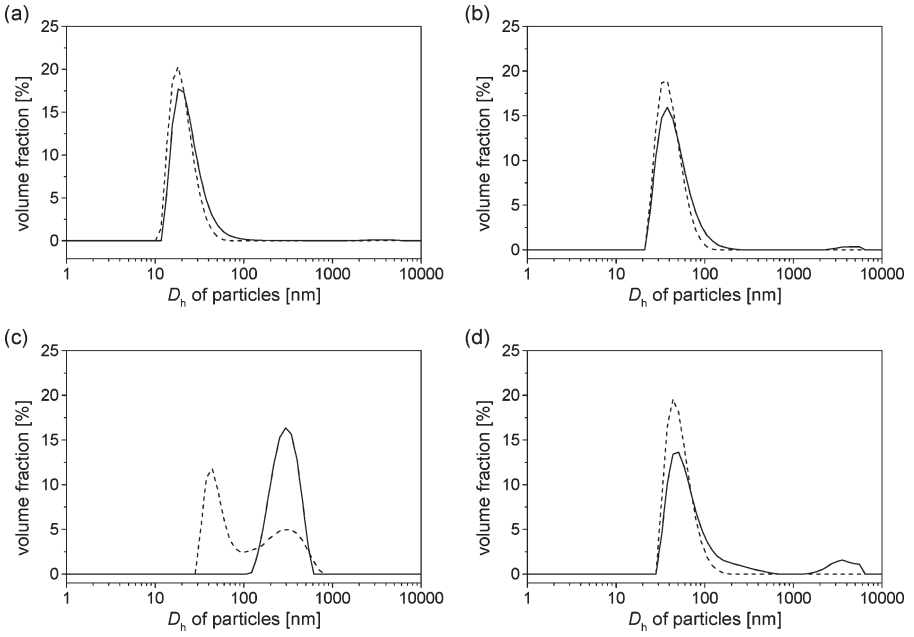

Figure 4. Particle size distributions of triblock copolymers (solid line) and of their precursor diblock copolymers (dashed line) in 0.5 wt % aqueous solutions as studied by DLS: (a) $(OEGA)_{70}$-$(BuA)_{83}$-$(FA)_{13}$; (b) $(OEGA)_{70}$-$(EHA)_{140}$-$(FA)_{13}$; (c) $(EHA)_{120}$-$(OEGA)_{50}$-$(FA)_{40}$; (d) $(EHA)_{120}$-$(OEGA)_{109}$-$(FA)_{25}$.

monomodal size distribution in most cases. The smaller size of the micelles made from diblock copolymers $(OEGA)_{70}$-$(BuA)_{83}$ and $(OEGA)_{70}$-$(FA)_{24}$ in comparison to $(OEGA)_{70}$-$(EHA)_{140}$, $(EHA)_{120}$-$(OEGA)_{50}$ and $(EHA)_{120}$-$(OEGA)_{109}$ is explained by the much larger hydrophobic blocks in the latter case. The bimodal size distribution in those cases where the block hydrophobicity is particularly high, i.e., $(OEGA)_{85}$-$(FA)_{24}$, $(EHA)_{120}$-$(OEGA)_{50}$, and $(EHA)_{120}$-$(OEGA)_{109}$ (see Figure 4), suggests that these systems are probably not fully equilibrated 1 day after preparation. Indeed, extended annealing reduces the fraction of the large particle population of $(EHA)_{120}$-$(OEGA)_{50}$ and $(EHA)_{120}$-$(OEGA)_{109}$. The larger particles with a mean particle diameter of several hundred nanometers cannot be explained by the formation of simple spherical micelles, as the contour length of the polymers is much too small. However, such large aggregates are frequently observed for block copolymers with long insoluble blocks and are attributed, for instance, to micellar clusters or large compound micelles formed by a secondary aggregation of primary micelles.[56,58]

The particle sizes and distributions appeared to be unaffected by aging, as the size analysis by DLS for the small aggregates were reproducible within experimental accuracy even after 2 weeks of storage (see Supporting Information, Table S2). Either equilibration between micelles is already attained 1 day after preparation or the exchange of macromolecules between the micelles is extremely slow. Although the absence of micelle equilibration for block copolymers

was originally attributed to the high T_g of the core-forming blocks used (PS or PMMA),[46,59] block copolymers comprising short hydrophobic blocks with a low T_g (PB) have been reported to form kinetically "frozen" micelles, too.[60,61] Hence, it cannot be decided whether the observed stability of the small particle size distributions is due to thermodynamic equilibrium or to kinetic effects, though the latter seem more probable.

In the case of the triblock copolymers, two groups can be distinguished. The first one comprises $(OEGA)_{70}$-$(BuA)_{83}$-$(FA)_{13}$ and $(OEGA)_{70}$-$(EHA)_{140}$-$(FA)_{13}$ and is characterized by the block sequence hydrophilic−lipophilic−fluorophilic. The second group comprises $(EHA)_{120}$-$(OEGA)_{50}$-$(FA)_{40}$ and $(EHA)_{120}$-$(OEGA)_{105}$-$(FA)_{25}$ and is characterized by the block sequence lipophilic−hydrophilic−fluorophilic. In the first group, the incorporation of the additional fluorinated block had no marked effect on the size distributions of the micelles compared to those of the corresponding diblock precursors (Figure 4a,b). The small changes of the particles sizes compared to the precursor diblock copolymer are consistent with the low degree of polymerization of the fluorinated blocks, which should hardly change the packing requirements for the overall hydrophobic parts. Noteworthy, the size distributions obtained when following protocol B for the self-assembly are very similar (see Supporting Information, Table S2).

In contrast, the addition of the fluorinated block has a bigger effect on the aggregates formed by the second group of triblock copolymers. While the size distribution is moderately increased in the case of $(EHA)_{120}$-$(OEGA)_{105}$-$(FA)_{25}$, i.e., the polymer with a longer hydrophilic middle block and a shorter fluorophilic end-block, the hydrodynamic diameters are markedly increased in the case of $(EHA)_{120}$-$(OEGA)_{50}$-$(FA)_{40}$ when following self-assembly protocol A (Figure 4c,d). Annealing for several weeks has only a minor effect on the size distributions. The measured average particle size of 240 nm is too large to correspond to the hydrodynamic diameter of a spherical micelle, as the contour length of the fully stretched polymer chain of $(EHA)_{120}$-$(OEGA)_{50}$-$(FA)_{40}$ is about 50 nm only. Therefore, larger aggregates such as micellar clusters must be formed. In fact, the self-assembly of symmetrical triblock polymers of the BAB type with hydrophobic end-blocks often results in the formation of interconnected micelles and networks. Still, when applying protocol B, the obtained aggregates are much smaller, though nonetheless being bigger than those obtained from the precursor diblock copolymer.

As for its diblock precursor, a second population of very large aggregates with dimensions larger than 1 μm was detected for copolymer $(EHA)_{120}$-$(OEGA)_{109}$-$(FA)_{25}$ (Figure 4d). As the large aggregates could not be removed by filtration prior to the DLS measurement, they might be attributed to clusters, which form by the interconnection of micelles via the hydrophobic end-blocks. In any case, the share of the aggregates decreases by annealing. Otherwise, the analysis of the micellar solutions after several weeks revealed virtually no changes of size or size distribution upon storage, so that the polymeric micelles appeared to be very stable. As discussed above for the diblock copolymers, it cannot be judged whether this stability results from approaching thermodynamic equilibrium or from frozen micellar exchange.

Micellar Morphologies Studied by Cryo-TEM. Whereas DLS provides only indirect access to the particle size and size distributions, cryo-TEM allows to image individual aggregates directly in the native state and thus to investigate the morphology and dimensions of the micelles formed in solution. Moreover, segregated fluorocarbon nanodomains can be visualized, as fluorocarbons are known to create high contrast in TEM.[25,27] Hence cryo-TEM has become the most powerful tool in the characterization of block copolymer micelles.[62]

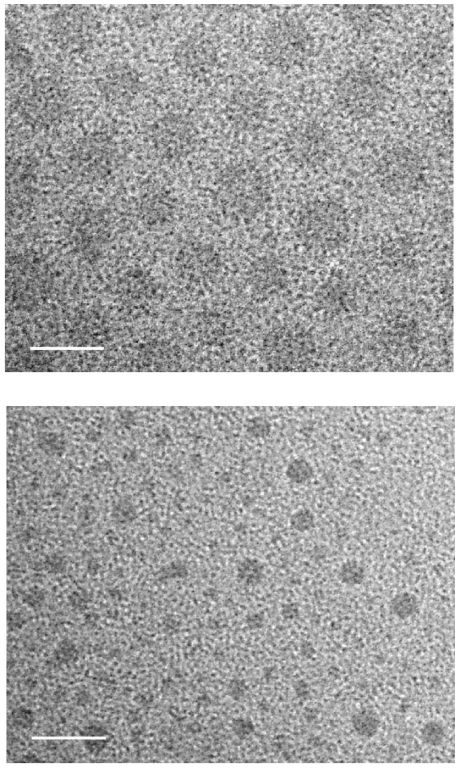

Figure 5. Exemplary cryo-TEM micrographs show micellar aggregates in 0.5 wt % aqueous solutions of the amphiphilic diblock copolymers: (a) $(EHA)_{120}$-$(OEGA)_{50}$; (b) $(OEGA)_{85}$-$(FA)_{24}$. Scale bar = 50 nm.

Precursor diblock copolymers were also included in the cryo-TEM studies in order to verify the formation of spherical micelles, which are usually anticipated for amphiphilic diblock copolymers. Additionally, cryo-TEM may also be helpful to clarify the origins of the bimodality observed for some diblock copolymer micelles by DLS. More importantly, the comparison of diblock and triblock copolymer micelles allows to better evaluate the impact of the fluorinated block on the micelle formation. For example, the incorporation of the fluorinated block might not only be accompanied by a change of the size and/or distribution of particles but might also induce a different micellar morphology.

Two examples for micellar aggregates formed by the amphiphilic diblock copolymers are depicted in Figure 5. Here, dark gray spheres represent the micellar cores made of polyEHA (Figure 5a) and polyFA (Figure 5b) with apparent core diameters of approximately 29 and 12 nm, respectively. As the electron density of well-solvated corona blocks is close to that of vitrified water, direct imaging of the corona is difficult.[62,63] In the present case, the corona can only be discerned in a few cases in the micrographs as a fringed seam surrounding the micellar core. This can be attributed to the compact bottlebrush-like conformation of the hydrophilic polyOEGA blocks, which appear with higher contrast under these conditions than a linear PEO chain.[64] Comparative cryo-TEM investigations on pure homopolymer $(OEGA)_{70}$ solutions revealed threadlike microstructures (see Supporting Information, Figure S3) and support the above finding.

In those cases where the corona cannot directly be visualized, its characteristic dimension may be derived from the

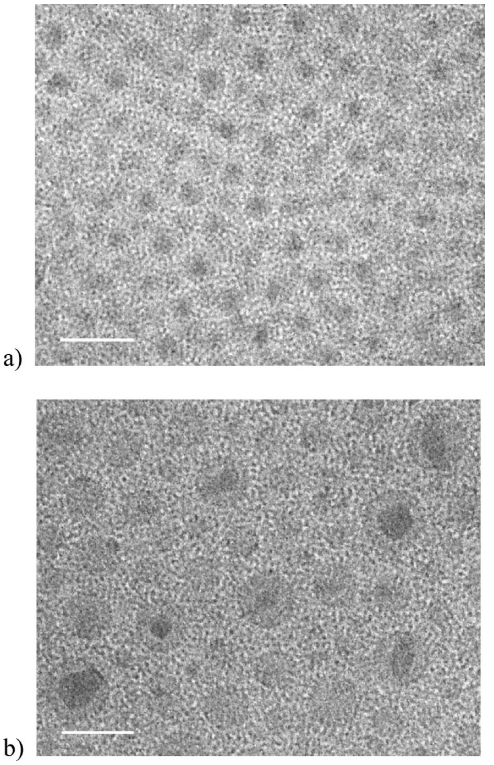

Figure 6. Cryo-TEM micrographs of micellar aggregates in 0.5 wt % aqueous solutions of amphiphilic triblock copolymers prepared at ambient conditions by protocol A: (a) $(OEGA)_{70}$-$(BuA)_{83}$-$(FA)_{13}$; (b) $(OEGA)_{70}$-$(EHA)_{140}$-$(FA)_{13}$. Scale bar = 50 nm.

micelles' core-to-core distance in the areas, where they are closely packed.[65] This enables the direct determination of the overall sizes of the micelles and allows comparing them to the results from DLS (Table 3). Both sets of values agree very well for the most part. Larger deviations occurred only for very small particles (~20 nm), for which the size measurements from the micrographs become increasingly difficult due to the inherent image noise.

DLS analysis revealed the presence of two populations of aggregates with hydrodynamic diameters of 55 and 300 nm, respectively, for diblock copolymer $(EHA)_{120}$-$(OEGA)_{50}$. As the measurements were performed at a zero degree tilt angle only, it could not be clarified whether the population of larger particles is due to isotropic or anisotropic structural effects. Cryo-TEM showed the presence of a few large spherical aggregates with core diameters ranging from 100 to 200 nm (see Supporting Information, Figure S4). This is in qualitative agreement with the DLS results. Large spherical objects are often found in aqueous solutions of amphiphilic block copolymers,[44,56,58] but it is not clear whether they are equilibrium structures or not. If they are true equilibrium structures, their occurrence could be possibly caused by the polydispersity of the block copolymers.

Cryo-TEM imaging of the micelles formed by the various triblock copolymers revealed characteristic features in dependence on the block sequence (Figures 6−9). Typical cryo-TEM images of micellar solutions for the sequence hydrophilic−lipophilic−fluorophilic block, which were prepared by protocol A, are shown in Figure 6. Both polymers $(OEGA)_{70}$-$(BuA)_{83}$-$(FA)_{13}$ and $(OEGA)_{70}$-$(EHA)_{140}$-$(FA)_{13}$ self-assemble into spherical micelles. In the case of $(OEGA)_{70}$-$(BuA)_{83}$-$(FA)_{13}$ (Figure 6a) the hydrophilic corona is visible as a fringed seam surrounding the high-contrast micellar core. In the case of $(OEGA)_{70}$-$(EHA)_{140}$-$(FA)_{13}$,

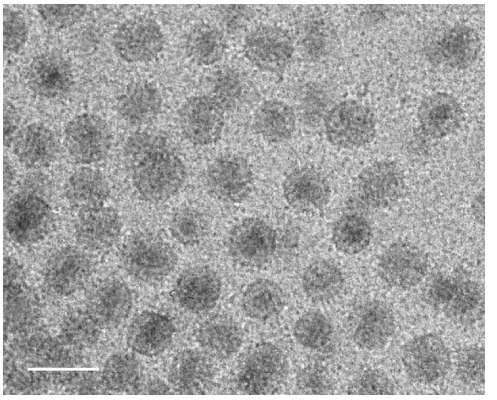

Figure 7. Cryo-TEM micrographs of micellar aggregates in 0.5 wt % aqueous solutions of triblock copolymer $(OEGA)_{70}$-$(BuA)_{83}$-$(FA)_{13}$ after thermal treatment (protocol C, i.e., preparation by protocol A and annealing for 25 days at 78 °C). Scale bar = 50 nm.

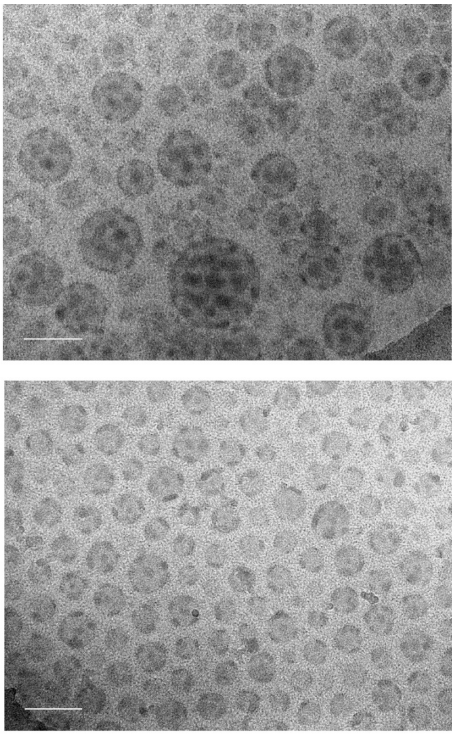

Figure 8. Cryo-TEM micrographs of micellar aggregates in 0.5 wt % aqueous solutions of triblock copolymer $(EHA)_{120}$-$(OEGA)_{50}$-$(FA)_{40}$: (a) dispersed at 25 °C (protocol A); (b) dispersed at 70 °C (protocol B). Scale bar = 100 nm.

additional dark patches are clearly visible within the micellar cores (Figure 6b), which can be attributed to microseparated fluorocarbon nanodomains.[25,27] Mostly, these domains appear spherical and to be arranged in concentric rings. Because of the specific architecture of these triphilic block copolymers, the mutual incompatibilities of the three blocks (cf. DSC studies, Table 2), and their interfacial tensions, a core−shell−corona morphology with segregated lipophilic and the fluorophilic domains can be expected. As contacts between the fluorinated domain and water are much less favorable than contacts between the lipophilic domain and water, the fluorinated domain should be buried in the inner part of the micelle. The block sequence hydrophilic−lipophilic−fluorophilic easily allows matching the geometric requirements. Although the cryo-TEM micrographs seem to support this model very well, it cannot be taken as a

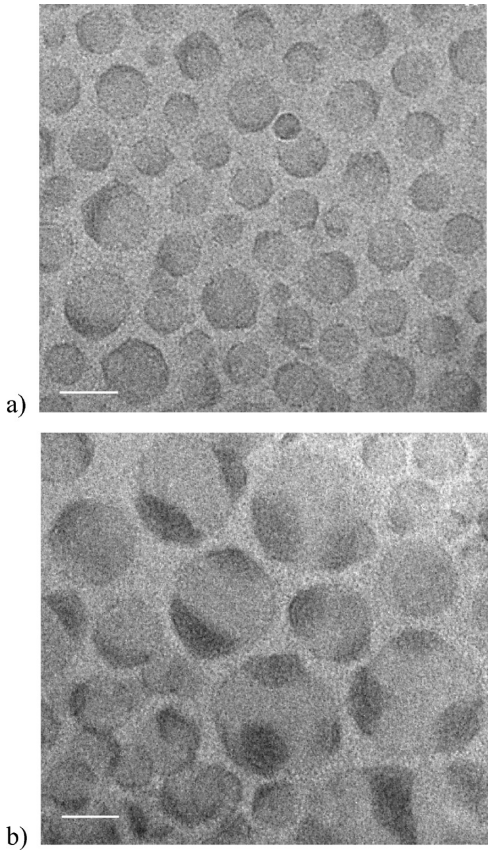

Figure 9. Cryo-TEM micrographs of micellar aggregates in 0.5 wt % aqueous solutions of triblock copolymer $(EHA)_{120}$-$(OEGA)_{109}$-$(FA)_{23}$. Morphologies after annealing for 25 days at 78 °C (protocol C): (a) smaller micelles showing mainly one single, caplike fluorinated domain surrounding a larger part of the spherical lipophilic core; (b) second population of larger aggregates showing a structure similar to the "soccer ball" morphology. Scale bar = 50 nm.

solid proof. One has to keep in mind that cryo-TEM provides only a two-dimensional (2D) projection of a three-dimensional (3D) object. Recently, we have shown that the spatial arrangement of fluorinated domains within the hydrocarbon core of a different block copolymer can be determined by employing cryogenic electron tomography (cryo-ET).[33] These data however confirmed the overall distribution of fluorinated domains in the hydrophobic core. Nevertheless, no fluorinated domain within the micellar aggregates of polymer $(OEGA)_{70}$-$(BuA)_{83}$-$(FA)_{13}$ could be directly assigned (Figure 6a), although the DSC studies indicate micro phase-separated lipophilic and fluorophilic blocks in bulk (cf. Table 2). This finding might be explained by the smaller micellar cores ($D_{core} \sim 16$ nm, cf. Table 3) in comparison to $(OEGA)_{70}$-$(EHA)_{140}$-$(FA)_{13}$ ($D_{core} \sim 28$ nm, cf. Table 3). Possibly, separate fluorocarbon microdomains occur in the micelles of $(OEGA)_{70}$-$(BuA)_{83}$-$(FA)_{13}$, too, but are smaller, so that they cannot be resolved.

Although the hydrophobic micellar cores of the aggregates of polymer $(OEGA)_{70}$-$(EHA)_{140}$-$(FA)_{13}$ appeared relatively uniform, their inner FC domains were irregularly shaped and showed a broad size distribution. While for some micelles no — or only minute — fluorinated domains were perceived, others contained large fluorinated cores. This finding could either owe to the polydispersity in molar mass and composition of the block copolymer or to a nonequilibrated state of polymeric micelles, as the crystallinity of the fluorinated block might prevent the equilibration of micellar structures. Therefore, a second series of micellar solutions were prepared above T_m (which is about 65 °C, cf. Table 2) of the fluorophilic block (protocol B) and studied by cryo-TEM. Additionally, the samples prepared according to protocol A were annealed at 78 °C for several days (protocol C) (Figure 7). It turned out that dispersion by protocol B hardly affected the morphology or the size and distribution of aggregates formed (not shown).

In contrast, while annealing at 78 °C did not notably affect the micelles formed by polymer $(OEGA)_{70}$-$(EHA)_{140}$-$(FA)_{13}$, the annealing at higher temperatures had a pronounced effect on the appearance of the micelles formed by $(OEGA)_{70}$-$(BuA)_{83}$-$(FA)_{13}$. The average diameter of micellar cores increased from about 16 nm to about 28 nm, and fluorinated microdomains become now clearly visible. Hence, a spherical core−shell−corona morphology may be deduced for this polymer, too, though it needs more time to evolve. The formation of core−shell−corona morphologies agree with earlier findings, by experiment[35,66] and by simulation,[11] that linear triphilic ABC block copolymers with a fluorophilic−lipophilic−hydrophilic block sequence tend to form micelles with a core−shell−corona morphology in water.

Subsequently, the micelles formed by the triphilic block copolymers with the alternative block sequence lipophilic−hydrophilic−fluorophilic were investigated by cryo-TEM. Typical micrographs of the micellar aggregates formed from $(EHA)_{120}$-$(OEGA)_{50}$-$(FA)_{40}$ and $(EHA)_{120}$-$(OEGA)_{109}$-$(FA)_{25}$ prepared by the various protocols are depicted in Figures 8 and 9. Indeed, the ultrastructures of the micelles formed differ strongly from the core−shell−corona morphology found for the block sequence hydrophilic−lipophilic−fluorophilic. Polymer $(EHA)_{120}$-$(OEGA)_{50}$-$(FA)_{40}$, which comprises the shorter hydrophilic central block, formed spherical micelles with microphase-separated lipophilic and fluorophilic domains reminiscent of a soccer ball. The fluorinated domains seem to be located as small disks predominately on the surface of the lipophilic micellar core. Such mutual arrangement could be expected because the fluorinated block is tethered to the corona-forming hydrophilic block. However, the fluorinated domains might be embedded within the lipophilic core, too. Cryo-TEM cannot clarify this issue as it yields only a 2D projection of 3D objects. Using cryoelectron tomography, it was possible to show that most of the fluorinated domains are located as well at the surface as deeply within the lipophilic core of larger micellar aggregates.[33] The latter are often organized in a tubelike manner, where the dense tube walls enclose a volume of lower density. Following Eisenberg's model of large compound micelles,[58] one could assume that they form inverse micelle-like aggregates, allowing the hydrophilic loops to be segregated from the hydrophobic environment. The generally flat morphology of the fluorinated domains might be the consequence of accessing the super-strong segregation regime and should be favored by the preferential lamellar packing of the crystallized fluorocarbon side chains of the polyFA block.[32,67]

Within this regime, the interfacial tension is so large that the fluorinated chains should tend to adopt a fully extended conformation in order to minimize the interfacial area per chain.[36,68] The typical thickness of the fluorocarbon nanodomains of 5−10 nm is in fact close to the contour length of the fluorinated block.

Although the micelles prepared by method A showed a broad size distribution with typical diameters ranging from 40 up to about 150 nm, the morphology and ultrastructure seem to be the same for all particle sizes. Because of the

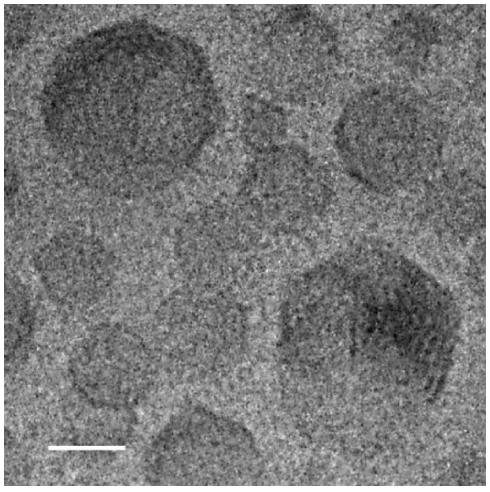

Figure 10. Cryo-TEM micrographs of micellar aggregates in 0.5 wt % aqueous solutions of triblock copolymer $(EHA)_{120}$-$(OEGA)_{109}$-$(FA)_{23}$: Morphologies after annealing for 25 days at 78 °C (protocol C) exhibit lattice fringes in the fluorinated domains. Scale bar = 30 nm.

solidlike fluorinated block, the polymeric micelles prepared from polymer $(EHA)_{120}$-$(OEGA)_{50}$-$(FA)_{40}$ at ambient conditions might be far from equilibrium. Nevertheless, annealing of the aqueous solutions at 78 °C had no visible effect on the morphology, size, or distribution of aggregates. In agreement with the DLS results (see Table 3 and also Supporting Information Table S3), however, the polymeric micelles prepared by method B were smaller, and their size distribution was narrower.

Polymer $(EHA)_{120}$-$(OEGA)_{109}$-$(FA)_{25}$ is made of the same monomer units and having the same block sequence, i.e., lipophilic−hydrophilic−fluorophilic, but contains a longer hydrophilic block as middle part than the above-discussed polymer. Cryo-TEM shows that preparation protocol A results in irregularly shaped spheroidal aggregates in addition to ribbonlike aggregates (see Supporting Information, Figure S5). These aggregates are obviously nonequilibrium structures. Whereas dispersing the polymer at 75 °C (protocol B) did not give much different results, dramatic changes of the morphology occurred upon annealing the solutions following protocol C. While the irregularly shaped and ribbonlike aggregates disappeared completely, spherical micelles with well-resolved fluorine domains emerged. Again, the size distribution is relatively broad. The smaller spherical micelles exhibited a core diameter of ∼40 nm. In contrast to the micelles of polymer $(EHA)_{120}$-$(OEGA)_{50}$-$(FA)_{40}$ with the shorter hydrophilic middle block, the set of smaller isolated fluorinated domains is replaced by one single, caplike domain surrounding a larger part of the spherical lipophilic core (Figure 9a). Located on the surface of the micellar cores, the fluorinated domains frequently displayed sharp edges (Figures 9 and 10). This finding points to the ability of the fluorinated domains to undergo crystalline ordering (see Table 2). This explanation is supported by the observation of lattice fringes in the cases of some larger micelles (Figure 10).

A second population of large aggregates that evolved upon annealing shows a structure, which is similar to the above-mentioned soccer ball morphology (see Figures 8 and 9b). Here, the remarkable structural feature is the existence of several fluorinated domains. With typical diameters up to 100 nm being much larger than the aggregates with a single FC domain, these aggregates are hypothesized to evolve by the fusion of smaller micelles.

If the respective block sizes are well chosen, linear triphilic block copolymers with three incompatible blocks and the block sequence lipophilic−hydrophilic−fluorophilic (BAC) can obviously aggregate into multicompartment core structures, too, instead of separate populations of micellar cores.[20,21,30,41] The found multicompartment structure of the cores resemble strongly to the "patched double micelles" theoretically predicted by de Gennes.[10] In these structures, hydrocarbon and fluorocarbon coexist in such a geometry that they share a common interface but also are both in direct contact with the aqueous phase. Such a geometry seems to be most suitable for the separate and independent solubilization of different substances in the respective compartments.[18,23,24,26]

Summary

Linear ternary block copolymers, which are composed of a hydrophilic, lipophilic, and fluorophilic block, can be synthesized in three successive polymerization steps by the RAFT method, with the possibility to vary the block sequence and without the need of protective groups. These "triphilic" polymers are able to aggregates in aqueous solution into small micelles with a multicompartment ultrastructure of the hydrophobic cores. Nonetheless, annealing steps may be helpful to develop the multicompartment structures as ultrastructure formation is kinetically controlled to a large extent. In particular, fluorophilic blocks containing long perfluoralkyl chains tend to facilitate microphase separation but also tend to crystallize, thus hampering rapid equilibration of the structures. In addition to the core−shell−corona morphology, some unprecedented new multicompartment morphologies were found, such as "patched double micelle" and larger "soccer ball" structures.

Importantly, the type of ultrastructure obtained depends sensitively on the block sequence as a characteristic molecular variable of linear block copolymers. The probably "intuitive" block sequence hydrophilic−lipophilic−fluorophilic, placing the most hydrophilic and the most hydrophobic blocks at opposite ends of the copolymers, provides micelles with core−shell−corona morphologies, with the fluorocarbon block forming the inner core. The core−shell−corona morphology is without doubt one elegant variety of different imaginable multicompartment structures, but seems nonideal, when different guest molecules are to be solubilized separately in the different compartments. As one hydrophobic compartment is enclosed in the other, the independent uptake of different solubilizates from and the release to the aqueous phase will be obstructed. Hence, when considering potential use of such multicompartment structures for purposes of selective solubilization, the block sequence lipophilic−hydrophilic−fluorophilic seems to be most promising, as "patched double micelles" multicompartment structures are formed. Here, the hydrocarbon and fluorocarbon domains coexist side by side and are both in direct contact with the aqueous phase. These structures should favor the independent uptake and release of different (and eventually incompatible) compounds, hence mimicking the diversified solubilization profile of blood transport proteins, as serum albumin.[69,70]

Acknowledgment. We thank E. Kleinpeter and M. Heydenreich (Universität Potsdam) for support with NMR measurements and M. Gräwert and H. Schlaad (MPI Colloids and Interfaces) and Ch. Wieland (Fraunhofer IAP) for support with SEC measurements. Financial support was provided by Deutsche Forschungsgemeinschaft (Grants LA 611/6 and BO 1000/8) and Fonds der Chemischen Industrie.

Supporting Information Available: Procedure for the synthesis of 2-(butylsulfanylthiocarbonylsulfanyl)propionic acid butyl ester (BTP) and full analytical data; tables of polymerization conditions for the synthesis of the triblock copolymers and

their precursors and of data from DLS analysis of homo- and block copolymer solutions (4.0 g/L) in THF and $CHCl_3$ as well as in water in dependence on storage period; differential scanning calorimetry traces of homopolymers $(OEGA)_{70}$, $(EHA)_{120}$, $(FA)_x$, and block copolymer $(EHA)_{120}$-$(OEGA)_{50}$-$(FA)_{40}$; ^1H NMR spectra of $(OEGA)_{70}$-$(BuA)_{140}$-$(FA)_{13}$ in $CDCl_3$ and in D_2O; cryo-TEM micrographs of aqueous solutions of $(OEGA)_{70}$ and of PEO, of large spherical objects occasionally observed for diblock copolymer $(EHA)_{120}$-$(OEGA)_{50}$, and of micellar aggregates of triblock copolymer $(EHA)_{120}$-$(OEGA)_{109}$-$(FA)_{23}$ prepared by protocol A. This material is available free of charge via the Internet at http://pubs.acs.org.

References and Notes

(1) Ringsdorf, H. 3rd EURESCO Conference on Supramolecular Chemistry: Molecular Recognition and Drug-Receptor Interactions, Salamanca, Spain, Aug 29−Sept 3, **1996**.
(2) Ringsdorf, H.; Lehmann, P.; Weberskirch, R. Multicompartmentation - a concept for the molecular architecture of life. Book of Abstracts, 217th ACS National Meeting, Anaheim, CA, March 21−25, **1999**.
(3) Laschewsky, A. *Curr. Opin. Colloid Interface Sci.* **2003**, *8*, 274–281.
(4) Lutz, J.-F.; Laschewsky, A. *Macromol. Chem. Phys.* **2005**, *206*, 813–817.
(5) Hamley, I. W. *Block Copolymers in Solution: Fundamentals and Applications*; John Wiley & Sons Ltd.: Chichester, England, 2005.
(6) Antonietti, M.; Förster, S. *Adv. Mater.* **2003**, *15*, 1323–1333.
(7) Lodge, T. P. *Macromol. Chem. Phys.* **2003**, *204*, 265–273.
(8) Cohen Stuart, M. A. *Colloid Polym. Sci.* **2008**, *286*, 855–864.
(9) Dormidontova, E. E.; Khokhlov, A. R. *Macromolecules* **1997**, *30*, 1980–1991.
(10) de Gennes, P. G. *C. R. Acad. Sci. Paris, Ser. IIb* **1999**, *327*, 535–538.
(11) Chou, S.-H.; Tsao, H.-K.; Sheng, Y.-J. *J. Chem. Phys.* **2006**, *125*, 194903.
(12) Xia, J.; Zhong, C. *Macromol. Rapid Commun.* **2006**, *27*, 1654–1659.
(13) Zhong, C.; Liu, D. *Macromol. Theory Simul.* **2007**, *16*, 141–157.
(14) Ma, J. W.; Li, X.; Tang, P.; Yang, Y. *J. Phys. Chem. B* **2007**, *111*, 1552–1558.
(15) Xia, J.; Liu, D.; Zhong, C. *Phys. Chem. Chem. Phys.* **2007**, *9*, 5267–5273.
(16) Zhulina, E. B.; Borisov, O. V. *Macromolecules* **2008**, *41*, 5934–5944.
(17) Ma, Z.; Jiang, W. *J. Polym. Sci., Part B: Polym. Phys.* **2009**, *47*, 484–492.
(18) Stähler, K.; Selb, J.; Candau, F. *Langmuir* **1999**, *15*, 7565–7576.
(19) Candau, F. *Macromol. Symp.* **2002**, *179*, 13–25.
(20) Kubowicz, S.; Thünemann, A. F.; Weberskirch, R.; Möhwald, H. *Langmuir* **2005**, *21*, 7214–7219.
(21) Weberskirch, R.; Preuschen, J.; Spiess, H. W.; Nuyken, O. *Macromol. Chem. Phys.* **2000**, *201*, 995–1007.
(22) Kotzev, A.; Laschewsky, A.; Rakotoaly, R. *Macromol. Chem. Phys.* **2001**, *202*, 3257–3267.
(23) Szczubialka, K.; Moczek, Ł.; Goliszek, A.; Nowakowska, M.; Kotzev, A.; Laschewsky, A. *J. Fluorine Chem.* **2005**, *126*, 1409–1418.
(24) Kotzev, A.; Laschewsky, A.; Adriaensens, P.; Gelan, J. *Macromolecules* **2002**, *35*, 1091–1101.
(25) Li, Z.; Kesselman, E.; Talmon, Y.; Hillmyer, M. A.; Lodge, T. P. *Science* **2004**, *306*, 98–101.
(26) Lodge, T. P.; Rasdal, A.; Li, Z.; Hillmyer, M. A. *J. Am. Chem. Soc.* **2005**, *127*, 17608–17609.
(27) Kubowicz, S.; Baussard, J.-F.; Lutz, J.-F.; Thünemann, A. F.; Berlepsch, H. v.; Laschewsky, A. *Angew. Chem., Int. Ed.* **2005**, *44*, 5262–5265.
(28) Thünemann, A. F.; Kubowicz, S.; Berlepsch, H. v.; Möhwald, H. *Langmuir* **2006**, *22*, 2506–2510.
(29) Li, Z.; Hillmyer, M. A.; Lodge, T. P. *Langmuir* **2006**, *22*, 9409–9417.
(30) Komenda, T.; Lüdtke, K.; Jordan, R.; Ivanova, R.; Bonné, T.; Papadakis, C. B. *Polym. Prepr.* (*Am. Chem. Soc., Div. Polym. Chem.*) **2006**, *47* (2), 763–764.
(31) Taribagil, R. R.; Hillmyer, M. A.; Lodge, T. P. *Macromolecules* **2009**, *42*, 1796–1800.
(32) Skrabania, K.; Laschewsky, A.; Berlepsch, H. v.; Böttcher, C. *Langmuir* **2009**, *25*, 7594–7601.
(33) Berlepsch, H. v.; Böttcher, C.; Skrabania, K.; Laschewsky, A. *Chem. Commun.* **2009**, 2290–2292.
(34) Kujawa, P.; Goh, C. C. E.; Calvet, D.; Winnik, F. M. *Macromolecules* **2001**, *34*, 6387–6395.
(35) Zhou, Z.; Li, Z.; Ren, Y.; Hillmyer, M. A.; Lodge, T. P. *J. Am. Chem. Soc.* **2003**, *125*, 10182–10183.
(36) Lodge, T. P.; Hillmyer, M. A.; Zhou, Z.; Talmon, Y. *Macromolecules* **2004**, *37*, 6680–6682.
(37) Li, Z.; Hillmyer, M. A.; Lodge, T. P. *Macromolecules* **2004**, *37*, 8933–8940.
(38) Li, Z.; Hillmyer, M. A.; Lodge, T. P. *Macromolecules* **2006**, *39*, 765–771.
(39) Fustin, C.-A.; Abetz, V.; Gohy, J.-F. *Eur. Phys. J. E* **2005**, *16*, 291–302.
(40) Ishizone, T.; Sugiyama, K.; Sakano, Y.; Mori, H.; Hirao, A.; Nakahama, S. *Polym. J. Jpn.* **1999**, *31*, 983–988.
(41) Shunmugam, R.; Smith, C. E.; Tew, G. N. *J. Polym. Sci., Part A: Polym. Chem.* **2007**, *45*, 2601–2608.
(42) Moad, G.; Rizzardo, E.; Thang, S. H. *Acc. Chem. Res.* **2008**, *41*, 1133–1142.
(43) Matyjaszewski, K.; Müller, A. H. E. *Controlled and Living Polymerizations. From Mechanisms to Applications*; Wiley-VCH: Weinheim, 2009.
(44) Cameron, N. S.; Corbierre, M. K.; Eisenberg, A. *Can. J. Chem.* **1999**, *77*, 1311–1326.
(45) Dormidontova, E. E. *Macromolecules* **1999**, *32*, 7630–7644.
(46) Riess, G. *Prog. Polym. Sci.* **2003**, *28*, 1107–1170.
(47) Garnier, S.; Laschewsky, A. *Macromolecules* **2005**, *38*, 7580–7592.
(48) Garnier, S.; Laschewsky, A. *Colloid Polym. Sci.* **2006**, *284*, 1243–1254.
(49) Lai, J. T.; Filla, D.; Shea, R. *Macromolecules* **2002**, *35*, 6754–6756.
(50) Bivigou-Koumba, A. M.; Kristen, J.; Laschewsky, A.; Müller-Buschbaum, P.; Papadakis, C. M. *Macromol. Chem. Phys.* **2009**, *210*, 565–578.
(51) Skrabania, K.; Li, W.; Laschewsky, A. *Macromol. Chem. Phys.* **2008**, *209*, 1389–1403.
(52) Favier, A.; Pichot, C. *Macromol. Rapid Commun.* **2006**, *27*, 653–692.
(53) Hirao, A.; Sugiyama, K.; Yokoyama, H. *Prog. Polym. Sci.* **2007**, *32*, 1393–1438.
(54) Mertoglu, M.; Laschewsky, A.; Skrabania, K.; Wieland, C. *Macromolecules* **2005**, *38*, 3601–3614.
(55) Petit, F.; Iliopoulos, I.; Audebert, R. *Polymer* **1998**, *39*, 751–753.
(56) Zhang, L.; Eisenberg, A. *Polym. Adv. Technol.* **1998**, *9*, 677–699.
(57) Shen, H.; Eisenberg, A. *J. Phys. Chem. B* **1999**, *103*, 9473–9487.
(58) Zhang, L.; Eisenberg, A. *J. Am. Chem. Soc.* **1996**, *118*, 3168–3181.
(59) Yu, G.-e.; Eisenberg, A. *Macromolecules* **1998**, *31*, 5546–5549.
(60) Won, Y.-Y.; Davis, H. T.; Bates, F. S. *Macromolecules* **2003**, *36*, 953–955.
(61) Meli, L.; Lodge, T. P. *Macromolecules* **2009**, *42*, 580–583.
(62) Cui, H.; Hodgdon, T. K.; Kaler, E. W.; Abezgauz, L.; Danino, D.; Lubovsky, M.; Talmon, Y.; Pochan, D. J. *Soft Matter* **2007**, *3*, 945–955.
(63) Zheng, Y.; Won, Y.-Y.; Bates, F. S.; Davis, H. T.; Scriven, L. E.; Talmon, Y. *J. Phys. Chem. B* **1999**, *103*, 10331–10334.
(64) Samokhina, L.; Schrinner, M.; Ballauff, M.; Drechsler, M. *Langmuir* **2007**, *23*, 3615–3619.
(65) Lin, E. K.; Gast, A. P. *Macromolecules* **1996**, *29*, 390–397.
(66) Gohy, J.-F.; Willet, N.; Varshney, S.; Zhang, J.-X.; Jérôme, R. *Angew. Chem., Int. Ed.* **2001**, *40*, 3214–3216.
(67) Shimizu, T.; Tanaka, Y.; Kutsumizu, S.; Yano, S. *Macromol. Symp.* **1994**, *82*, 173–184.
(68) Semenov, A. N.; Nyrkova, I. A.; Khokhlov, A. R. *Macromolecules* **1995**, *28*, 7491–7500.
(69) Kragh-Hansen, U. *Pharmacol. Rev.* **1981**, *33*, 17–53.
(70) Carter, D. C.; Ho, J. X. *Adv. Protein Chem.* **1994**, *45*, 153–203.